molecular pharmaceutics

Article

pubs.acs.org/molecularpharmaceutics

Neoglycolipids for Prolonging the Effects of Peptides: Self-Assembling Glucagon-like Peptide 1 Analogues with Albumin Binding Properties and Potent in Vivo Efficacy

Søren B. van Witteloostuijn,[†,‡] Karin Mannerstedt,[†] Pernille Wismann,[†,§] Esben M. Bech,[†,‡] Mikkel B. Thygesen,[‡] Niels Vrang,[†] Jacob Jelsing,[†] Knud J. Jensen,[*,‡] and Søren L. Pedersen[*,†]

[†]Gubra ApS, Hørsholm Kongevej 11B, 2970 Hørsholm, Denmark

[‡]Department of Chemistry, Faculty of Science, University of Copenhagen, Thorvaldsensvej 40, 1871 Frederiksberg C, Denmark

[§]Department of Clinical Medicine, Faculty of Health Science, University of Copenhagen, Blegdamsvej 9, 2100 København Ø, Denmark

S *Supporting Information*

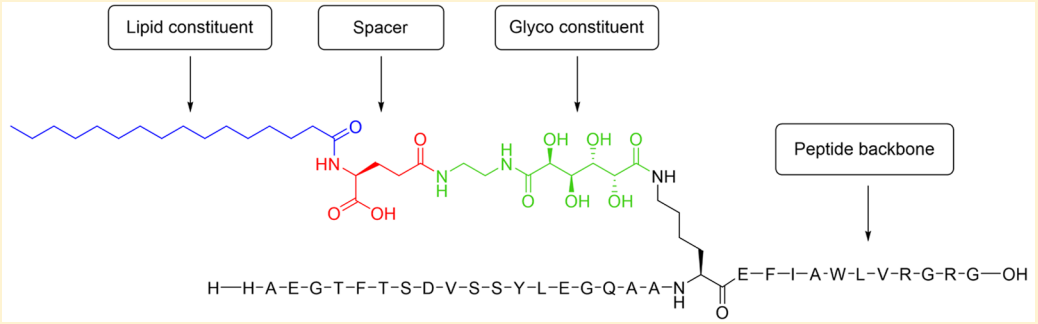

ABSTRACT: Novel principles for optimizing the properties of peptide-based drugs are needed in order to leverage their full pharmacological potential. We present the design, synthesis, and evaluation of a library of neoglycolipidated glucagon-like peptide 1 (GLP-1) analogues, which are valuable drug candidates for treatment of type 2 diabetes and obesity. Neoglycolipidation of GLP-1 balanced the lipophilicity, directed formation of soluble oligomers, and mediated albumin binding. Moreover, neoglycolipidation did not compromise bioactivity, as in vitro potency of neoglycolipidated GLP-1 analogues was maintained or even improved compared to native GLP-1. This translated into pronounced in vivo efficacy in terms of both decreased acute food intake and improved glucose homeostasis in mice. Thus, we propose neoglycolipidation as a novel, general method for modulating the properties of therapeutic peptides.

KEYWORDS: *neoglycolipid, lipidation, glucagon-like peptide 1, glycolipid, half-life extension, biopharmaceutical, peptide*

INTRODUCTION

During the past 30 years, biopharmaceuticals have become increasingly important for the treatment of a variety of diseases, including several cancer forms, inflammatory disease, diabetes, and obesity. The combined annual revenue of the more than 200 approved drug products has reached 140 billion USD.[1] Due to their endogenous origin, biopharmaceuticals are usually highly selective and potent compounds. However, since they are based on native polypeptides, they suffer from rapid proteolytic degradation and, in the case of peptides and smaller proteins, susceptibility to renal clearance. This often results in very short in vivo half-lives that are incompatible with a meaningful dosing regimen.

To compensate for poor pharmacokinetic properties, a variety of half-life extension techniques have been developed.[2,3] Peptides and to a lesser extent proteins have been chemically modified at their side-chains to introduce groups that modify their pharmacokinetic properties without inhibiting receptor binding and activation.[4,5] One of the most widely adapted chemical modifications of biopharmaceutical peptides and proteins has been the introduction of large poly(ethylene glycol) (PEG) groups, a process that is referred to as PEGylation. Conjugation of large PEG polymers increases the hydrodynamic radius of the modified peptide or protein,[6] thereby rendering it less susceptible to renal clearance and more resistant toward protease degradation.[7,8] Despite the commercial success of PEGylated biopharmaceuticals, the potential safety concerns associated with the unnatural PEG polymers remain a matter of debate.[9,10] Moreover, most large PEGs are not monodisperse, leading to polydisperse PEGylated proteins. Finally, PEGylation significantly increases the

Received: August 25, 2016
Revised: November 4, 2016
Accepted: December 1, 2016
Published: December 1, 2016

DOI: 10.1021/acs.molpharmaceut.6b00787
Mol. Pharmaceutics XXXX, XXX, XXX−XXX

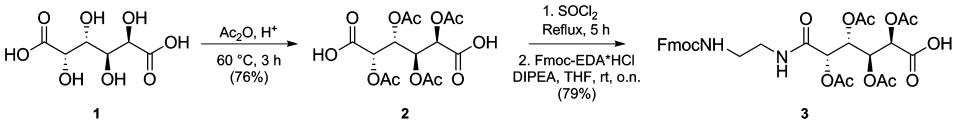

Figure 1. Synthesis of Fmoc-Muc-OH.

molecular mass of the target biopharmaceutical, which may complicate formulation of high doses suitable for subcutaneous (sc) administration.

Another technology that enhances the pharmacokinetic properties of peptides and proteins is lipidation with long-chain fatty acids. This approach has successfully been used by Novo Nordisk in two long-acting insulins (insulin detemir and insulin degludec) and two glucagon-like peptide 1 (GLP-1) analogues (liraglutide and semaglutide).[11−14] Half-life extension arises from noncovalent anchoring of peptides and proteins to the fatty acid binding sites on human serum albumin (HSA).[15−17] When bound to HSA, renal clearance is reduced and proteolytic degradation is minimized due to steric effects. Moreover, introduction of fatty acids can induce self-assembly of the modified polypeptides,[11,12,18] thereby effectively forming an in vivo sc depot resulting in delayed absorption. However, lipidation increases the overall lipophilicity of the native polypeptide, and this may lead to solubility issues, especially for very long fatty acids such as stearic acid and arachidic acid. Incorporation of a hydrophilic spacer between the lipid and the polypeptide has been used to compensate for the overall decrease in water solubility. γ-L-Glutamic acid (γGlu) has been used extensively and successfully for this purpose, both alone[12,13,19−23] and in combination with the short PEG-type spacer 8-amino-3,6-dioxaoctanoic acid (O2Oc) such as in semaglutide.[14]

We hypothesized that carbohydrates inserted between the peptide side chain and the lipid moiety could modulate the physicochemical properties of biopharmaceuticals in novel ways. Carbohydrates are often hydrophilic due to the number of hydroxyl groups, they have a large structural diversity, their chemistry is very well-described, and many carbohydrates are easily available. In general, short carbohydrates (mono- and oligosaccharides) show a low degree of immunogenicity. Some carbohydrates are used as excipients to prevent aggregation and to increase the solubility of polypeptides. Furthermore, glycolipids such as octyl β-D-glucopyranoside are widely used detergents for the solubilization of integral membrane proteins.[24]

A lipid−carbohydrate−peptide conjugate can also be viewed as a peptide modified by a glycolipid; as a non-natural glycolipid it is termed a neoglycolipid. We hypothesized that covalently anchored neoglycolipids could constitute a new class of half-life extending moieties for peptides and proteins, allowing binding to albumin and directing oligomerization in the nanoscale in the absence of albumin. Here, we focused on open-chain monosaccharide derivatives.

To validate the effects of neoglycolipidation in a biopharmaceutical context, we chose GLP-1 as the first target. GLP-1 is a peptide hormone secreted from the gut in response to food ingestion. In the periphery, GLP-1 actions include amplification of pancreatic insulin secretion (the "incretin effect"), inhibition of glucagon secretion, stimulation of beta cell proliferation, and inhibition of gastric acid secretion, intestinal motility, and gastric emptying (the "enterogastrone effect"). In addition, GLP-1 acts centrally to inhibit food intake and appetite.[25] The physiology of GLP-1 makes this peptide a very important target for the treatment of metabolic syndrome, and several GLP-1 analogues are approved or in clinical development for the treatment of type 2 diabetes as well as obesity.[26,27]

We present the design and synthesis of novel neoglycolipids based on an open-chain sugar amino acid as well as the synthesis of a library of neoglycolipidated GLP-1 analogues. We show that neoglycolipidation directs self-assembly of the peptide conjugate and mediates binding to HSA. Compared to native GLP-1, the neoglycolipidated GLP-1 analogues had the same or even improved in vitro potency. This translates into superior in vivo efficacy with respect to reducing acute food intake and improving glucose homeostasis in lean mice.

RESULTS

Design and Synthesis of Neoglycolipidated GLP-1 Analogues. In the neoglycolipid design, we focused on optimizing in vitro potency and physicochemical properties of the target peptide while maintaining albumin binding and ensuring in vivo efficacy. As glycoconstituent, we chose mucic acid (**1**), a commercially available aldaric acid obtained by oxidation of galactose. To incorporate mucic acid into peptides by established solid-phase methods, the aldaric acid was converted into an amino acid building block amenable to Fmoc-based solid-phase peptide synthesis (SPPS). The first step was protection of the hydroxyl groups of mucic acid by acid-catalyzed acetylation to yield the corresponding tetraacetate (**2**) (Figure 1). The second step was incorporation of Fmoc-protected ethylenediamine (Fmoc-EDA) to provide an Fmoc-protected amino functionality. We first explored direct coupling of Fmoc-EDA and mucic acid tetraacetate using standard reagents for amide bond formation, but generation of significant amounts of the disubstituted byproduct made this approach unattractive. Instead, we synthesized the acid chloride, which upon amidation with Fmoc-EDA provided the monosubstituted sugar amino acid (**3**) (named Fmoc-Muc-OH) in acceptable yield (Figure 1). This carbohydrate-based amino acid is directly compatible with Fmoc-SPPS and can be anchored to *N*-terminal or side-chain peptide amino groups by an amide bond. Moreover, multiple Muc units can be coupled sequentially, thereby providing neoglycolipids with carbohydrate moieties of different size.

The commercially available fatty acids palmitic acid (C16), stearic acid (C18), and arachidic acid (C20) were used to synthesize neoglycolipids containing fatty acids of different lengths. Fatty acids are directly compatible with Fmoc-SPPS and may be readily incorporated into peptides using standard solid-phase conditions.

The target peptide of choice, GLP-1, circulates in two forms: an amidated variant known as GLP-1(7−36)-NH_2 (**4**) and a Gly-extended variant termed GLP-1(7−37)-OH, with the amidated form being predominant in humans.[25] A slightly modified form of GLP-1(7−37)-OH, termed [Arg34]GLP-1(7−37)-OH (**5**), constitutes the peptide backbone of the well-characterized GLP-1 analogue liraglutide (**7**), which in addition

DOI: 10.1021/acs.molpharmaceut.6b00787
Mol. Pharmaceutics XXXX, XXX, XXX−XXX

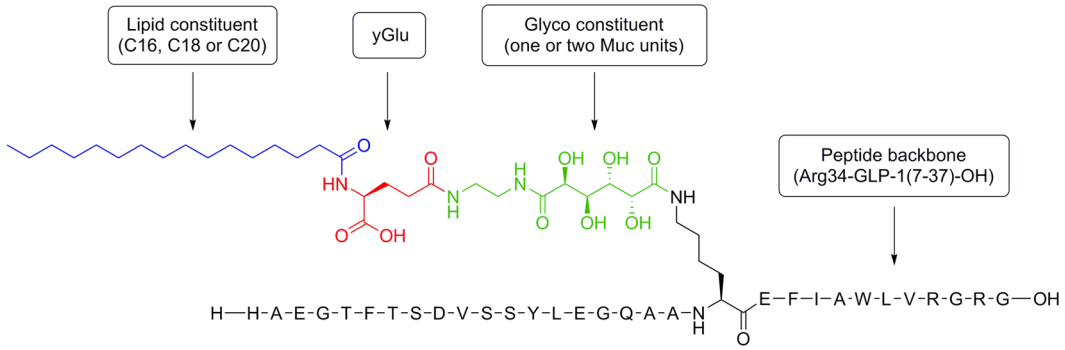

Figure 2. Architecture of neoglycolipidated peptides exemplified by compound **8** (neoglycolipid variant: C16-γGlu-Muc-). The lipid constituent is marked in blue, γGlu is marked in red, the glyco constituent is marked in green, and the peptide backbone is marked in black (with Lys26 expanded for clarity).

to the K34R mutation is modified at the side chain of Lys26 with a γGlu-spaced palmitic acid (C16-γGlu-).[13] Lys26 in peptide **5** was identified as an optimal lipidation site during the development of liraglutide (**7**).[28] Thus, we used this position for neoglycolipidation. In addition to the carbohydrate and lipid moieties, a γGlu unit was also included in the neoglycolipid design, since the presence of this amino acid is known to have positive effects on albumin binding. Importantly, this allowed direct comparison with liraglutide (**7**), when studying the impact of neoglycolipidation on peptide properties.

A series of neoglycolipidated peptides was prepared by Fmoc-SPPS. C-terminal peptide acids were obtained by SPPS on a TentaGel resin with a 4-alkoxybenzyl alcohol (PHB) linker and the first Gly anchored as the ester. Site-specific lipidation at the side chain of Lys26 was achieved by selective removal of the orthogonal Alloc protecting group using $(PPh_3)_4Pd(0)$, followed by on-resin assembly of the neoglycolipids using standard coupling reagents. Neoglycolipidated peptides containing acetyl-protected carbohydrate moieties were released from the solid support, purified by preparative RP-HPLC, and lyophilized. The acetyl protecting groups were subsequently removed in solution using $NaOCH_3$ in CH_3OH, and the final products were obtained by a second round of preparative RP-HPLC (Figures 2, S1). All peptides were analyzed by LC−MS. In total, six neoglycolipidated peptides (compounds **8**−**13**) were prepared (Table 1). In addition, the des-γGlu version of liraglutide (**6**) and a version containing O2Oc as part of the spacer (**14**) were synthesized as reference compounds.

Functional Screening. To assess the impact of neoglycolipidation on functional activity, the in vitro potency of all compounds was investigated using a human embryonic kidney (HEK293) cell line expressing the EPAC cAMP-sensor and the GLP-1 receptor (GLP-1R). The dose−response curves of all compounds are shown in Figure 3, and the derived EC_{50} values are listed in Table 1. All compounds were full GLP-1R agonists, with EC_{50} values in the picomolar range. The most potent compound was **11** (C16-γGlu-Muc-Muc-, EC_{50} = 13.4 ± 1.8 pM), with potency gradually declining for **12** (C18-γGlu-Muc-Muc-, EC_{50} = 16.8 ± 2.3 pM) and **13** (C20-γGlu-Muc-Muc-, EC_{50} = 41.2 ± 4.2 pM). The same trend was observed for compounds **8**−**10**, suggesting that increasing fatty acid length moderately interferes with receptor activation, possibly due to steric effects. Moreover, compounds **11**−**13** were generally more potent than compounds **8**−**10**, suggesting that increasing the distance between the peptide backbone and the lipid moiety was beneficial for receptor activation. With the exception of **10** (C20-γGlu-Muc-, EC_{50} = 118.8 ± 28.2 pM), all neoglycolipidated peptides were equipotent with or even more potent than liraglutide (**7**, C16-γGlu-, EC_{50} = 63.6 ± 6.4 pM), suggesting that inclusion of an extra carbohydrate moiety as part of the spacer gave optimal interaction between peptide and receptor. A comparison of **8** (C16-γGlu-Muc-, EC_{50} = 21.8 ± 2.5 pM) and **14** (C16-γGlu-O2Oc-, EC_{50} = 35.9 ± 3.7 pM) suggests that our carbohydrate-based spacer compared favorably with the O2Oc moiety in terms of maintaining compound potency.

Table 1. Glycolipid Variant and Functional Screening Data for the Library of Neoglycolipidated GLP-1 Analogues[a]

compd no.	glycolipid variant	EC_{50} (pM) GLP-1R
4 (GLP-1(7−36)-NH_2)	n/a	41.2 ± 3.9
5 ([Arg34]GLP-1(7−37)-OH)	n/a	64.1 ± 4.5
6	C16-	67.8 ± 7.6
7 (liraglutide)	C16-γGlu-	63.6 ± 6.4
8	C16-γGlu-Muc-	21.8 ± 2.5
9	C18-γGlu-Muc-	44.1 ± 2.0
10	C20-γGlu-Muc-	118.8 ± 28.2
11	C16-γGlu-Muc-Muc-	13.4 ± 1.8
12	C18-γGlu-Muc-Muc-	16.8 ± 2.3
13	C20-γGlu-Muc-Muc-	41.2 ± 4.2
14	C16-γGlu-O2Oc-	35.9 ± 3.7

[a]All lipidated and neoglycolipidated peptides were functionalized at position Lys26 (bold) of [Arg34]GLP-1(7-37)-OH, H-HAEGTFTS-DVSSYLEGQAA**K**EFIAWLVRGRG-OH. EC_{50} values are presented as mean ± SEM derived from three independent experiments carried out in triplicate (n = 3).

Physicochemical Properties. *Peptide Lipophilicity.* In a first attempt to assess the impact of neoglycolipidation on peptide properties, the interaction between the neoglycolipidated peptides and an analytical C18 column was studied by UPLC. The presence of organic solvents ensured that the peptides were evaluated on their monomeric form. Column retention times (t_R) for compounds **5**−**14** are listed in Table 2. As expected, the interaction between the neoglycolipidated peptides and the column material is primarily governed by the length of the fatty acid, with longer fatty acids providing a longer retention time (as exemplified by compounds **8**−**10** and **11**−**13**, respectively). The pronounced difference in retention time for **6** (C16, t_R = 12.3 min) and liraglutide (**7**, C16-γGlu-, t_R = 7.7 min) illustrates the contribution of the γGlu spacer to peptide lipophilicity. Inclusion of one Muc unit provides an

DOI: 10.1021/acs.molpharmaceut.6b00787
Mol. Pharmaceutics XXXX, XXX, XXX−XXX

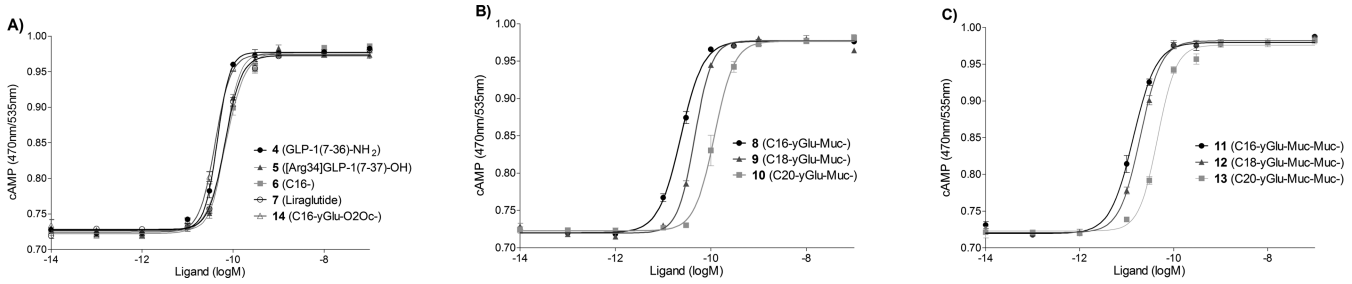

Figure 3. In vitro dose−response relationship of compounds **4**−**14** on GLP-1R. Functional activity of all compounds was investigated using a HEK293 cell line expressing the EPAC cAMP-sensor and the GLP-1R. (A) Compounds **4**−**6**, liraglutide (**7**), and **14**. (B) Compounds **8**−**10**. (C) Compounds **11**−**13**. Data are presented as mean ± SEM of three independent experiments carried out in triplicate (n = 3).

Table 2. Physicochemical Properties of Compounds 5−14[a]

compd no.	glycolipid variant	t_R (min)	max. solubility (mg mL^{-1})
5	n/a	2.7	1.4
6	C16-	12.3	1.2
7 (liraglutide)	C16-γGlu-	7.7	2.6
8	C16-γGlu-Muc-	6.1	2.6
9	C18-γGlu-Muc-	10.3	1.6
10	C20-γGlu-Muc-	21.8	2.6
11	C16-γGlu-Muc-Muc-	5.9	nd
12	C18-γGlu-Muc-Muc-	10.4	1.1
13	C20-γGlu-Muc-Muc-	21.8	1.0
14	C16-γGlu-O2Oc-	7.0	2.4

[a]Estimate of hydrophilicity is provided as the maximal solubility in PBS (pH 7.4). Estimate of hydrophobicity is provided as retention time following isocratic elution from an analytical C18 column.

additional decrease in retention time (**8**, C16-γGlu-Muc-, t_R = 6.1 min), whereas incorporation of a second Muc unit seems to have almost no additional effect (**11**, C16-γGlu-Muc-Muc-, t_R = 5.9 min). A comparison of **8** and **14** (C16-γGlu-O2Oc-, t_R = 7.0 min) suggests that the O2Oc moiety is more lipophilic than Muc, emphasizing the hydrophilic nature of the carbohydrate-based building block. The very short retention time of **5** (t_R = 2.7 min) may be attributed to a very low lipophilicity of the peptide backbone itself.

Peptide Solubility. The effect of neoglycolipidation on peptide solubility was estimated by the maximal solubility of compounds **5**−**14** under aqueous conditions. Compounds were dissolved in PBS (pH 7.4) until a saturated solution was obtained. The samples were centrifuged, and the absorbance at 280 nm was measured and used to calculate the peptide content of the supernatant, which was used as a measure of maximal solubility (Table 2). The low solubility of **5** (1.4 mg mL^{-1}) indicates that the unmodified peptide backbone has a low intrinsic solubility. A slight decrease in solubility is observed upon incorporation of palmitic acid (**6**, C16-, 1.2 mg mL^{-1}), whereas inclusion of a γGlu spacer potently improves solubility (liraglutide, **7**, C16-γGlu-, 2.6 mg mL^{-1}). Inclusion of Muc or O2Oc did not increase solubility beyond 2.6 mg mL^{-1}.

Size Exclusion Chromatography. As molecular self-assembly may affect solubility properties, and since it has been reported that some lipidated peptides form soluble oligomers, the oligomeric states of the neoglycolipidated peptides at concentrations of maximal solubility were investigated. The apparent molecular weights of compounds **5**−**14** were determined by size exclusion chromatography (SEC) using a Superdex 75 column. Figure 4 depicts the retention volumes (V_R) of compounds **5**−**14**, and the derived apparent molecular weights and oligomeric states (m) are listed in Table 3. Rewardingly, with the exception of **5** and **6**, all compounds eluted as single peaks, indicating the presence of uniform particle sizes. The retention volumes of the two peaks observed for **5** indicated the presence of two species with apparent molecular weights of 1.9 and 5.3 kDa, respectively (corresponding to m = 0.6 and m = 1.6, respectively), indicating a monomer−dimer distribution. The single peaks observed for compounds liraglutide (**7**) and **8**−**14** all have retention

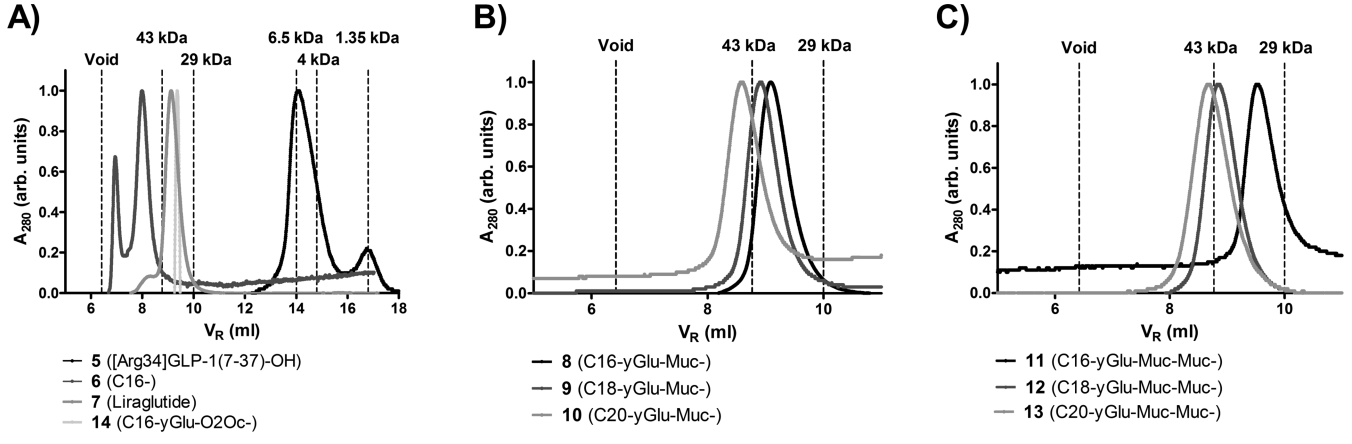

Figure 4. Estimation of apparent molecular weight of compounds **5**−**14** by SEC. V_R of MW standards is indicated by vertical dashed lines. (A) Compounds **5**, **6**, liraglutide (**7**), and **14**. (B) Compounds **8**−**10**. (C) Compounds **11**−**13**.

DOI: 10.1021/acs.molpharmaceut.6b00787
Mol. Pharmaceutics XXXX, XXX, XXX−XXX

Table 3. Retention Volume, Apparent Molecular Weight, and Oligomeric State of Compounds 5−14 and Hydrodynamic Radius and Polydispersity Index of Compounds 7−10[a]

		SEC			DLS	
compd no.	glycolipid variant	V_R (mL)	app MW (kDa)	m	r_H (nm)	PI
5	n/a	16.4/14.0	1.9/5.3	0.6/1.6	nd	nd
6	C16-	8.0/6.1	nd[b]	nd[b]	nd	nd
7 (liraglutide)	C16-γGlu-	9.1	43.4	11.6	9.6 ± 0.56	0.21 ± 0.01
8	C16-γGlu-Muc-	9.1	43.4	10.9	7.7 ± 0.17	0.29 ± 0.02
9	C18-γGlu-Muc-	8.9	47.2	11.8	23.2 ± 1.5	0.20 ± 0.008
10	C20-γGlu-Muc-	8.6	53.7	13.3	7.8 ± 0.28	0.24 ± 0.008
11	C16-γGlu-Muc-Muc-	9.5[b]	36.5[c]	8.7	nd	nd
12	C18-γGlu-Muc-Muc-	8.9	47.2	11.1	nd	nd
13	C20-γGlu-Muc-Muc-	8.7	53.7	12.6	nd	nd
14	C16-γGlu-O2Oc-	9.4	38.1	9.8	nd	nd

[a]Apparent molecular weight and oligomeric state were determined by SEC using a linear calibration curve, whereas hydrodynamic radius was determined by DLS and reported as the value derived from the data fit generated by second-order cumulant analysis. The values of hydrodynamic radius and the polydispersity index are presented as mean ± SEM, n = 4−8. [b]Peaks eluted outside the range of the calibration curve. [c]Sample concentration was below maximal solubility.

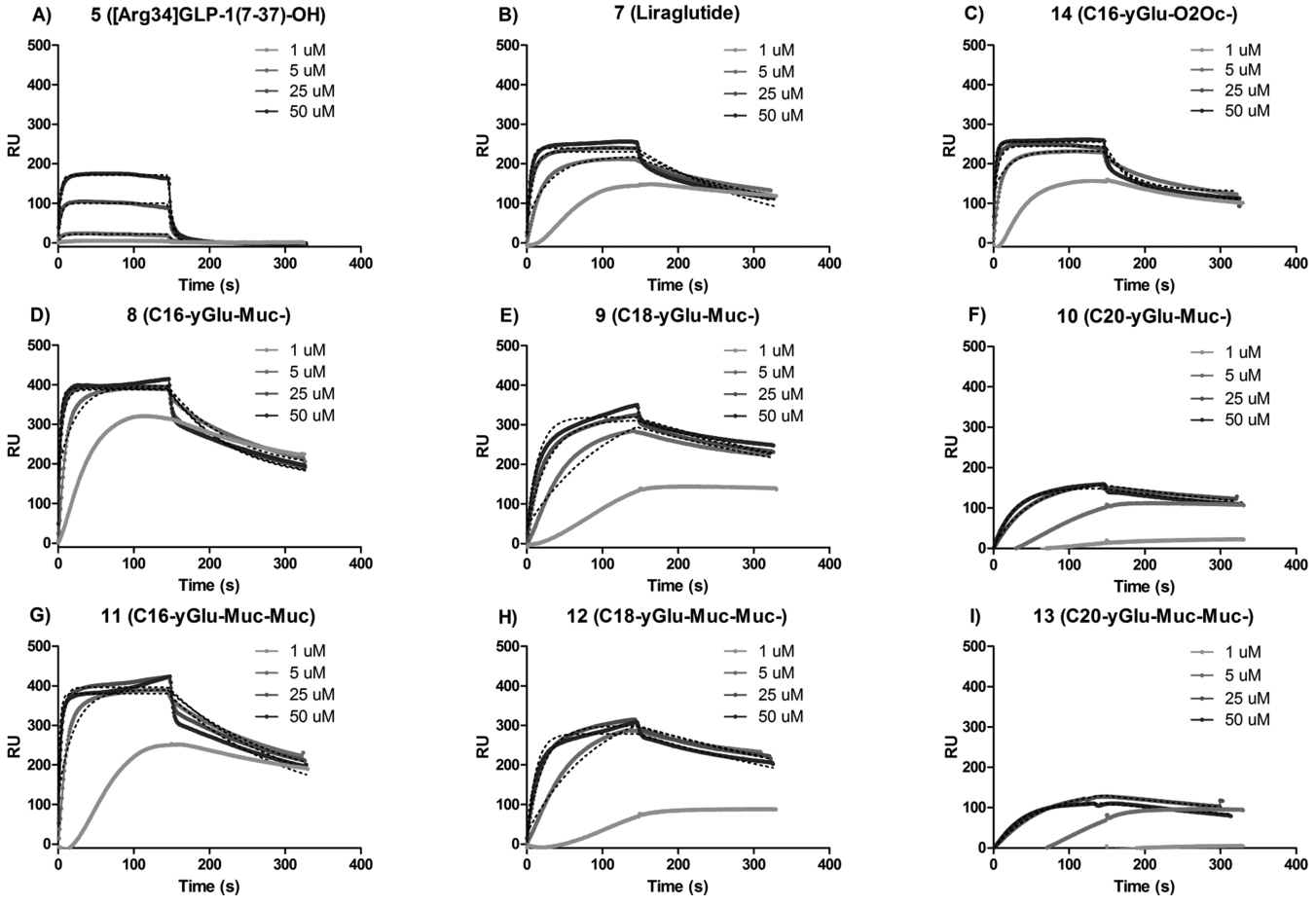

Figure 5. Sensorgrams showing interaction between immobilized HSA and compounds **5** and **7−14**. Analytes were injected for 150 s, followed by injection of running buffer for 180 s. Data are presented as mean ± SEM of triplicate injections from a single representative experiment. Data fits by nonlinear regression are depicted as dotted lines.

volumes of 8.6−9.5 mL, corresponding to apparent molecular weights of approximately 35−55 kDa (m = 8.7−13.3), suggesting that these compounds assemble into oligomeric structures containing between 9 and 13 monomer subunits, respectively. Interestingly, compared to lipidation with the C16-γGlu- motif, neoglycolipidation seems to direct formation of slightly smaller oligomers, as indicated by, e.g., the oligomeric state of liraglutide (**7**), **8**, and **11** (m = 11.16, m = 10.9, and m = 8.7, respectively). In addition, increasing fatty acid length results in formation of larger oligomeric structures, as evident by the oligomeric state of, e.g., compounds **11−13** (Figure 4C, m = 8.7 for C16, m = 11.1 for C18, and m = 12.6 for C20, respectively).

DOI: 10.1021/acs.molpharmaceut.6b00787
Mol. Pharmaceutics XXXX, XXX, XXX−XXX

Dynamic Light Scattering. In addition to the apparent molecular weight derived from SEC, the hydrodynamic radius (r_H) was determined for liraglutide (**7**) and a subset of the neoglycolipidated peptides (compounds **8**−**10**) by dynamic light scattering (DLS) (Table 3). For all four compounds, data fitting using a regularization algorithm indicated the presence of monodisperse solutions (data not shown), allowing r_H to be determined using second-order cumulant analysis. All compounds exhibited narrow size distributions, as indicated by low polydispersity indexes (PI). The reported values of r_H are consistent with oligomer formation.[29] The similar hydrodynamic radii of liraglutide (**7**), **8**, and **10** (r_H = 9.6 nm, r_H = 7.7 nm, and r_H = 7.8 nm, respectively) reflects the similarity of the oligomeric states (m = 11.6, m = 10.9, and m = 13.3, respectively) derived from SEC. The significantly greater hydrodynamic radius of **9** (r_H = 23.2 nm) may be attributed to the presence of a small amount of very large oligomers, which are detectable only by DLS and not by SEC.

Albumin Binding. In order to estimate the albumin binding propensity of the neoglycolipidated peptides, we investigated the interaction between immobilized HSA and neoglycolipidated peptides in solution using surface plasmon resonance (SPR) based detection on a Biacore X100 instrument. HSA was immobilized on Biacore CM5 chips, and analyte solutions containing peptides **5** and **7**−**14** were passed over the chip surface. Under conditions of total internal reflection, the changes in SPR response were measured during association and dissociation of the analytes. Figure 5 shows representative sensorgrams obtained for compounds **5** and **7**−**14**. Under the chosen assay conditions, all peptides exhibited reversible albumin binding, as indicated by the increase and decrease in response units (RU) during sample and buffer injections, respectively (Figure 5). Peptide **5** displayed very rapid association and dissociation kinetics with a calculated equilibrium dissociation constant, K_D, of 28.5 μM, suggesting that the unmodified peptide backbone interacts with HSA in a highly dynamic manner. Peptides **7**−**14** also displayed fast association kinetics. However, the dissociation rates for these compounds were much lower than that of **5**, indicative of a vastly enhanced affinity toward albumin. Saturation of the chip surface for these compounds was apparent at 25 μM or in some cases even at 5 μM. At analyte concentrations of 1 μM or lower, the association phases of compounds **7**−**14** displayed delayed, sigmoidal onsets of surface interaction, thus precluding straightforward analyses at low analyte concentrations (Figure 5). Variations in flow rate or level of immobilized HSA did not improve the data (data not shown). Due to the inadequate binding curves obtained at 1 μM, binding analyses had to be based on analyte concentration of 5, 25, and 50 μM, at or close to saturating conditions. Association kinetics at these analyte concentrations were too fast for proper estimation of the corresponding association rate constants, k_a, likely leading to gross underestimation. On the other hand, saturating conditions should not affect the dissociation rate constants, k_d. The release of analyte from the immobilized ligand, i.e., albumin, in the dissociation phase is in most kinetic models described by a simple monoexponential function. Thus, we found that the k_d values could be used as a simple measure for evaluating albumin binding of neoglycolipidated peptides. Table 4 lists the observed saturation response levels (R_{max}) as well as calculated k_d values for compounds **5** and **7**−**14**. The values of $k_{a,app}$ and $K_{D,app}$ are reported in Table S1.

Table 4. Saturation Response Levels (R_{max}) and Dissociation Rate Constants (k_d) Obtained for the Interaction of Neoglycolipidated Peptides with Immobilized HSA[a]

compd no.	glycolipid variant	R_{max} (RU)	k_d (s^{-1})
5	n/a	nd	0.1664 ± 0.0024
7 (liraglutide)	C16-γGlu-	250	0.0056 ± 0.00040
8	C16-γGlu-Muc-	400	0.0094 ± 0.0027
9	C18-γGlu-Muc-	320	0.0024 ± 0.00035
10	C20-γGlu-Muc-	150	0.0019 ± 0.00015
11	C16-γGlu-Muc-Muc-	400	0.0081 ± 0.0018
12	C18-γGlu-Muc-Muc-	300	0.0020 ± 0.000014
13	C20-γGlu-Muc-Muc-	120	0.00089 ± 0.00062
14	C16-γGlu-O2Oc-	260	0.026 ± 0.0005

[a]Data are presented as mean ± SEM of triplicate injections of two independent measurements (n = 2) conducted on the same chip.

In Vivo Pharmacology. *Acute Effect on Glucose Tolerance.* Since one of the most important pharmacological effects of GLP-1 analogues is their ability to decrease blood glucose levels and improve glycemic control, we evaluated the glucose lowering effects of compounds **8**−**10** in lean mice during an oral glucose tolerance test (OGTT) using liraglutide (**7**) as positive control (Figure 6). Compounds were injected 45 min prior to the oral glucose load (t = 0), and blood glucose levels were measured at 0, 30, 60, 90, and 120 min after administration of the glucose load. Administration of neoglycolipidated peptides **8**−**10** improved glucose tolerance by 50−62% (assessed as total AUC during OGTT, $p < 0.001$ vs vehicle), while administration of liraglutide (**7**) provided a 54% improvement ($p < 0.001$ vs vehicle).

Acute Effect on Food Intake. In addition to the beneficial effects on glucose homeostasis, administration of liraglutide and other GLP-1 analogues is also known to decrease food intake in rodents as well as humans. As such, we also investigated the anorectic effect of compounds **8**, **9**, **11**, and **12** in lean mice (Figure 7). Compounds were administered as a single dose, and food intake was measured for 18 h postdosing using a fully automated HerdsMan-2 (HM-2) food intake monitoring system, which enables advanced synchronous real-time monitoring of the feeding behavior of individual animals. Administration of neoglycolipidated peptides **8**, **9**, **11**, and **12** potently reduced cumulative food intake by 47−55% ($p < 0.001$ versus vehicle), whereas liraglutide (**7**) decreased food intake by 45% ($p < 0.001$ versus vehicle).

DISCUSSION

In the present study, we describe the development and characterization of neoglycolipidated GLP-1 analogues. The neoglycolipidation motif was designed to modulate peptide properties by inducing molecular self-assembly and prolonging plasma half-life via noncovalent albumin binding, while minimizing the decrease in solubility that is often observed with current lipidation strategies. Rewardingly, neoglycolipidation of GLP-1 occurred without compromising bioactivity, as the in vitro potency and in vivo efficacy were sustained. Importantly, neoglycolipidation decreased lipophilicity and provided noncovalent oligomerization. Neoglycolipidation represents a novel principle for directing self-assembly of therapeutic peptides. This feature is significant, since self-assembly has been suggested as one of the main reasons for the delayed absorption of liraglutide and insulin degludec and is

DOI: 10.1021/acs.molpharmaceut.6b00787
Mol. Pharmaceutics XXXX, XXX, XXX−XXX

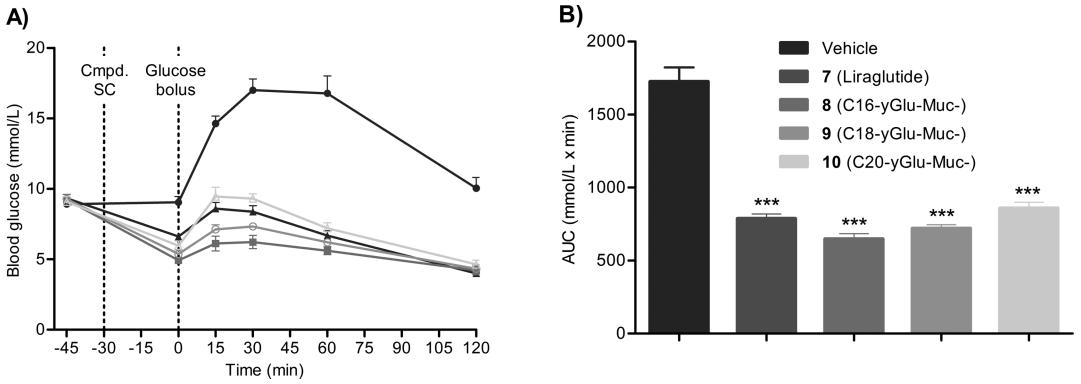

Figure 6. Evaluation of the glucose lowering potential of liraglutide (**7**) and compounds **8**−**10** in an OGTT. Compounds were administered (sc 50 nmol kg^{-1}) at t = −45 min, and glucose was dosed (per oral, 2 g/kg) at t = 0. Mice were semifasted for 5 h before the glucose load. (A) Glucose time−response curve (−45 to 120 min). (B) Area under the curve (AUC_{0-120}). Data presented as mean ± SEM, n = 7. Statistical analysis: one-way ANOVA with Bonferroni's post test against vehicle (***p < 0.001 versus vehicle).

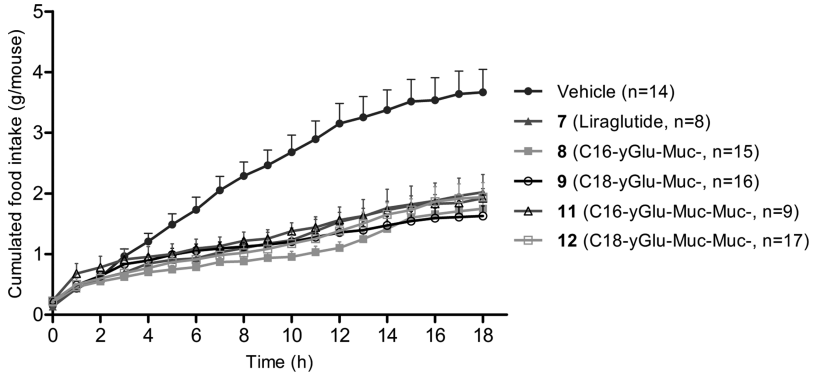

Figure 7. Cumulated food intake following acute single-dose administration (sc, 50 nmol kg^{-1}) of liraglutide (**7**) and compounds **8**, **9**, **11**, and **12** to lean mice. Food intake was monitored for 18 h postdosing using a fully automated HM-2 system. For each group, data was obtained from two independent studies and pooled to increase statistical power. Statistical analysis: one-way ANOVA with Dunnett's multiple comparison test (***p < 0.001 versus vehicle). Data presented as mean ± SEM, n = 8−17.

recognized as an important contributor to the prolonged half-life observed with these lipidated biopharmaceuticals.[12,18]

In a first attempt to evaluate the impact of neoglycolipidation on the physicochemical properties of peptides, the lipophilicity of the neoglycolipidated peptides was estimated. Although this parameter is primarily influenced by fatty acid length, incorporation of a carbohydrate-based amino acid did provide a decrease in lipophilicity, in terms of a shorter column retention time. In contrast to our initial expectations, this decrease in lipophilicity did not translate into improved solubility, as the inclusion of a carbohydrate moiety in the spacer did not increase the maximal aqueous solubility beyond that of liraglutide (**7**). The exact reason for this remains unknown, but the negative charge of the γGlu unit is known to contribute significantly to the solubility of other lipidated peptides.[20,23,28] As alternative to Muc, a carbohydrate moiety derived from e.g. glucuronic acid or sialic acid can be envisioned. Both of these species carry negative charges, and this may improve solubility even further.

Another important solubility driver is the ability of lipidated peptides to undergo self-assembly and form oligomers that remain in solution. This has previously been shown for both insulin degludec[12] and liraglutide.[18] Using SEC, we demonstrate the ability of neoglycolipidated peptides to form soluble oligomers in a size range of 35−55 kDa, corresponding to oligomers containing 9−13 peptide subunits. The amphiphilic nature of the neoglycolipidated peptides makes it likely that they self-assemble into micelle-like structures; however, this has not yet been studied. A similar assembly has been suggested for liraglutide oligomers.[29]

The oligomeric state of liraglutide has been determined using complementary techniques. Using analytical ultracentrifugation, Steensgaard et al. showed that at pH 8.0 liraglutide assembles into an aggregate with molecular weight of 25.9 kDa, corresponding to a heptameric structure (m = 6.9). Heptamer formation was observed in the concentration range of 0.001−1.2 mM, suggesting that the critical micelle concentration (CMC) is ≤1 μM.[18] Wang et al. used a combination of DLS and static light scattering (SLS) to investigate liraglutide self-assembly as a function of pH. In 20 mM sodium phosphate buffer at pH 7.4, DLS revealed that liraglutide undergoes oligomer formation in a well-defined manner, as indicated by a narrow size distribution. The r_H of the oligomers was 2.8 ± 0.1 nm. Using SLS, the molecular weight of the oligomers was calculated to 30 ± 2 kDa, which corresponds to an octamer (m = 8.0 ± 0.4).[29] SEC revealed a well-defined oligomerization of liraglutide, as indicated by the presence of a single narrow peak.

Using a calibration curve derived from well-defined molecular weight standards, we calculated the size of the liraglutide oligomers to 43.4 kDa, corresponding to a 12-mer (m = 11.6) at pH 7.4. The reason for the discrepancy between this value and previously reported values has not yet been fully

DOI: 10.1021/acs.molpharmaceut.6b00787
Mol. Pharmaceutics XXXX, XXX, XXX−XXX

clarified, but Wang et al. showed that the degree of oligomerization is strongly dependent on the pH value of the surrounding buffer (with m increasing from 8.0 ± 0.4 at pH 7.4 to 12.0 ± 0.6 at pH 6.7),[29] indicating that minute differences in the chemical environment of the different experimental setups could account for the different observations. This notion is supported by biophysical studies conducted by Clodfelter et al. on an octanoylated GLP-1 analogue, which illustrated that the oligomerization process was strongly solvent, temperature, and time dependent.[30]

Although albumin binding via lipidation is a well-established method for prolonging peptide half-life in vivo, a robust in vitro assay able to directly measure albumin affinity of lipidated peptides in a screening setup has proven difficult to develop. Kurtzhals et al. investigated albumin binding of insulin detemir and other lipidated insulin analogues using an ultrafiltration-based assay with albumin immobilized to an agarose matrix,[15] and Plum et al. developed an optimized equilibrium dialysis method and used it to determine the free fraction of liraglutide in the presence of albumin.[31] However, the requirement for radiolabeled ligands for both of these assays makes them less feasible for screening purposes. In a recent publication, Lau et al. estimated albumin binding of lipidated GLP-1 analogues by measuring binding to the GLP-1 receptor in the presence of albumin, using the ratio of IC_{50} values obtained with 0% and 2% HSA, respectively, as a surrogate of albumin affinity.[14] This indirect assay is more appropriate for a screening setup, but is not suitable for ligands with a strong affinity for both albumin and the corresponding receptor.

In contrast, SPR-based techniques such as Biacore require no labeling and provide a direct measure of the interaction between ligand and albumin. A drawback associated with this method is the need for immobilization of albumin, which may cause inadvertent steric occlusion of binding sites. However, this effect is compensated by the fact that immobilization is performed randomly at surface-exposed lysine residues, and that albumin contains multiple fatty acid binding sites. Using a Biacore assay for albumin binding, we observed reversible association and dissociation phases for liraglutide (**7**) and peptides **8**−**14** (Figure 5). However, binding analyses were complicated by apparent sigmoidal association curves at low analyte concentrations, as well as rapid onsets of binding saturation, thus precluding straightforward determination of binding constants (K_D). This could be due to an unspecific component in the binding interactions, in which some lipidated peptides may be irreversibly bound to surfaces in the instrument. Nonetheless, the albumin binding propensity of the neoglycolipidated peptides could be evaluated from the determined values of k_d and R_{max} at the higher concentrations.

Clearly, the most important factor governing albumin binding kinetics is the length of the fatty acid moieties. This may be observed directly from the sensorgrams, e.g., by comparison of Figures 5D−F, and is also reflected in the reported k_d values, indicating stronger albumin affinities for peptides containing longer fatty acids (Table 4). Interestingly, it seems that increasing fatty acid length decreases not only dissociation rates but also the corresponding association rates, suggesting that the length of the fatty acid impacts both the way the analyte approaches and binds the immobilized HSA and its subsequent release from HSA.

Surprisingly, we did not observe similar values of R_{max} for neoglycolipidated peptides with approximately identical molecular mass, for example, for compounds **8**−**10** or **11**−**13**. Given that the neoglycolipidated peptides undergo self-assembly, a possible explanation could be that peptide oligomers are present in the samples, resulting in a competing monomer−oligomer equilibrium during the association phase that apparently secludes the interaction between neoglycolipidated peptides and immobilized albumin.

Interestingly, the observed R_{max} values correlate closely with the determined oligomeric state of compounds liraglutide (**7**) and **8**−**14**, given in Table 3. For example, the saturation response of compound **13**, carrying a C20 fatty acid and displaying an oligomeric state of 12.0, amounted to only half that of compound **11** carrying a C16 fatty acid with an oligomeric state of 8.4 (Figures 5I and 5G, respectively).

Importantly, neoglycolipidated peptides carrying one or two Muc units in the spacer, e.g., compounds **8** and **11**, respectively, provided a more pronounced interaction with albumin, as judged by the higher R_{max} relative to liraglutide (**7**), while maintaining similar dissociation rate constants. While the additional Muc unit in compound **11** relative to **8** seems to have little effect on the binding kinetics (Figure 5G versus 5D), it is interesting that the hydrophilic nature of the Muc unit relative to the oligoethylene glycol O2Oc moiety of compound **14** is responsible for the enhancement of albumin interaction.

Functional screening of the neoglycolipidated GLP-1 analogues revealed that all compounds were full GLP-1R agonists and had maintained potency in the picomolar range, suggesting that neoglycolipidation did not interfere with receptor activation. Although lipidation of GLP-1 at Lys26 is known to be well-tolerated, the molecular composition of the spacer must be carefully designed to avoid disrupting the receptor interaction.[13,14,28] Rewardingly, inclusion of a mucic acid based moiety in the neoglycolipid design did not harm GLP-1R agonism, and the maintained in vitro potency translated into pronounced in vivo efficacy, as indicated by the improvement of glucose tolerance and potent reduction of food intake following acute administration of neoglycolipidated GLP-1 analogues. This validated our choice of Lys26 for lipidation.

The data on acute food intake (Figure 7) clearly demonstrate that the duration of action of compounds **8**, **9**, **11**, and **12** equals that of liraglutide (**7**), suggesting that the half-life of the neoglycolipidated GLP-1 analogues resembles that of liraglutide and is compatible with once-daily dosing in man. Thus, the desired extension of the function of neoglycolipidated peptides was achieved and we did not determine the PK profile of the neoglycolipidated peptides separately.

■ CONCLUSION

In summary, we have described the design of a novel neoglycolipid motif based on an open-chain sugar amino acid and the synthesis of an ensemble of neoglycolipidated GLP-1 analogues. Neoglycolipidation reduces peptide lipophilicity, maintains solubility, and mediates albumin binding. Introduction of the neoglycolipid motif directs formation of soluble peptide oligomers of variable size, depending on the chemical composition of the neoglycolipid. Neoglycolipidation of GLP-1 resulted in maintained or even improved in vitro potency compared to native GLP-1, which translated into potent in vivo efficacy. Acute administration of neoglycolipidated GLP-1 analogues improved glucose tolerance in lean mice, and the neoglycolipidated peptides exhibited a duration of action similar to that of liraglutide in terms of reducing food intake.

DOI: 10.1021/acs.molpharmaceut.6b00787
Mol. Pharmaceutics XXXX, XXX, XXX−XXX

We suggest neoglycolipidation as a novel principle for modulating the properties of therapeutic peptides.

EXPERIMENTAL SECTION

General Procedures. Peptides were purified by preparative RP-HPLC on a C18 column (Gemini-NX 5μ, 110 Å, 100 × 21.2 mm, Phenomenex) using a Waters 150 LC system equipped with a UV detector and a solvent system consisting of buffer A (0.1% TFA in H_2O) and buffer B (0.1% TFA in CH_3CN). Crude acetylated peptides were eluted from the column using a 10−60% linear gradient of buffer B (0−27 min, 10−60%; 27−30 min, 60−100%; flow rate, 30 mL min^{-1}). Deacetylated peptides were eluted from the column using a 30−50% linear gradient of buffer B (0−1 min, 10%; 1−2 min, 10−30%; 2−27 min, 30−50%; 27−30 min, 50−100%; 30 mL min^{-1}). RP-HPLC fractions were quantified by LC−MS using a Waters XEVO SQD instrument equipped with a C18 analytical column (Acquity UPLC BEH Amide column, 1.7 μm, 130 Å, 2.1 mm × 100 mm, Waters) and a solvent system consisting of buffer C (95% H_2O, 5% CH_3CN, 0.1% HCOOH) and buffer D (95% CH_3CN, 5% H_2O, 0.1% HCOOH). Peptides were eluted from the column using a linear gradient of buffer D (0−6 min, 0−100%; flow, 0.5 mL min^{-1}). NMR spectra were recorded on a Bruker 300 (300 MHz for ^1H, 75 MHz for ^{13}C) equipped with a BBO probe using either CH_3OH-d_4 or CH_3CN-d_3 as solvent. Chemical shifts are reported in parts per million (ppm) (δ relative to tetramethylsilane (TMS)). Statistical analysis, data fitting, and data plotting were performed using GraphPad software (GraphPad Prism version 5.04 for Windows, San Diego, CA, USA).

Materials. Liraglutide (**7**) was purchased as Victoza (6 mg mL^{-1} formulation) and either used as such (for in vivo studies) or purified by preparative RP-HPLC prior to use (for functional screening and studies of physicochemical properties). Fmoc-protected amino acids, ethyl (hydroxyimino)cyanoacetate (OxymaPure), *N*,*N*′-diisopropylcarbodiimide (DIC), piperidine, *N*,*N*-diisopropylethylamine (DIPEA), TFA, *N*-methyl-2-pyrrolidone (NMP), and DMF were purchased from Iris Biotech GmbH (Marktredwitz, Germany). Mucic acid, concentrated H_2SO_4, $SOCl_2$, THF, CH_2Cl_2, palmitic acid (C16), stearic acid (C18), arachidic acid (C20), TES, Et_2O, CH_3CN, $NaOCH_3$ (0.5 M) in CH_3OH, CH_3COOH, HCOOH, $(PPh_3)_4Pd(0)$, borane dimethylamine complex, 4-(2-hydroxyethyl)-1-piperazineethanesulfonic acid (HEPES), HSA (fatty acid free), $MgCl_2$, $CaCl_2$, BSA, and cell dissociation solution (nonenzymatic) were purchased from Sigma-Aldrich (Denmark). Zeocin and geneticin were purchased from Invitrogen (Thermo Fisher Scientific, Denmark). Growth medium (Dulbecco's modified Eagle medium (DMEM) with glutaMAX-I and 4.5 g/L D-glucose), fetal bovine serum (FBS), penicillin and streptomycin, geneticin (G418), PBS (pH 7.4), PBS without $CaCl_2$ and $MgCl_2$, and Hanks balanced salt solution (HBSS) were purchased from Gibco (Denmark). 384-Well format black sterile microplates were purchased from BD Falcon (USA). Excitation filter CFP 430/24 (X430), emission filters FITC 535/25 (M535), and CFP 470/24 (M470) as well as a CFP/YFP D450_515 single mirror were purchased and placed in an Envision 2104 Multilabel Reader (PerkinElmer, USA). Milli-Q water (Merck Millipore) was used for all experiments

Synthesis of Mucic Acid Tetraacetate (2).[32] Acetic anhydride (35 mL) and concentrated H_2SO_4 (5 drops) were added to mucic acid (**1**, 5.0 g, 23.8 mmol) in a round-bottom flask followed by heating at 60 °C for 3 h. After the reaction mixture was cooled to room temperature, H_2O (20 mL) was added and the mixture was stirred at 0 °C for 1 h. The product was filtered, washed with H_2O (20 mL), and dried to give a white solid (6.80 g, 17.99 mmol, 76%): ^1H NMR (300 MHz, CH_3OH-d_4) δ 5.70 (s, 2H), 5.15 (s, 2H), 2.15 (s, 6H), 2.05 (s, 6H); ^{13}C NMR (75 MHz, CH_3OH-d_4) δ 171.65, 170.55, 170.12, 70.74, 69.60, 20.40, 20.32.

Synthesis of (2*S*,3*R*,4*S*,5*R*)-6-((2-(*N*-Fmoc)aminoethyl)-amino)-2,3,4,5-tetraacetoxy-6-oxohexanoic Acid (Fmoc-Muc-OH, 3). Mucic acid tetraacetate (**2**, 1.0 g, 2.64 mmol) and $SOCl_2$ (30 mL) were heated to reflux for 5 h. The reaction mixture was cooled down and evaporated to give the acid chloride as a pale yellow solid. The product was used without further purification. The acid chloride (2.64 mmol) was dissolved in THF (10 mL), followed by addition of DIPEA (2 mL). Fmoc-EDA·HCl (0.42 g, 1.32 mmol) in THF (10 mL) were added dropwise, and the reaction mixture was stirred at room temperature overnight. The solvent was evaporated and the residue redissolved in CH_2Cl_2 (50 mL), washed with 1 M HCl (2 × 20 mL) and brine (30 mL), dried with Na_2SO_4, and evaporated. The product was precipitated by dissolving the residue in a small amount of CH_3OH (1 mL) and thereafter adding Et_2O (50 mL) during stirring. The mixture was left in the fridge overnight, and the solid was filtered and dried to give a white solid (0.669 g, 1.04 mmol, 79%): ^1H NMR (CH_3CN-d_3) δ 7.84 (d, J = 7.3 Hz, 2H), 7.66 (d, J = 7.5 Hz, 2H), 7.43 (t, J = 7.5 Hz, 2H), 7.34 (t, J = 7.5 Hz, 2H), 7.06 (s, 1H), 5.76 (s, 1H), 5.56 (s, 2H), 5.14 (s, 1H), 5.06 (s, 1H), 4.34 (d, J = 6.7 Hz, 2H), 4.23 (t, J = 6.8 Hz, 2H), 3.27−3.08 (m, 4H), 2.14 (s, 3H), 2.08 (s, 3H), 1.99 (s, 3H), 1.97 (s, 3H); ^{13}C NMR (CH_3CN-d_3) δ 170.84, 170.14, 168.39, 167.82, 157.89, 145.19, 142.14, 128.69, 128.12, 126.14, 120.97, 71.91, 70.34, 69.43, 68.84, 67.13, 48.10, 40.98, 40.52, 21.02, 20.69, 20.60; ESI-MS m/z calculated for $C_{31}H_{34}N_2O_{13}$ $[M + H]^+$ 643.61, found 643.4.

Peptide Synthesis. The [Arg34,Lys26(All)]GLP-1(7−37)-OH peptide backbone was prepared by automated peptide synthesis on a Syro II peptide synthesizer (MultiSynTech, Witten, Germany; Biotage AB, Uppsala, Sweden) by Fmoc-SPPS. Peptide synthesis was conducted on a 0.1 mmol scale using Fmoc Gly TentaGel S PHB resin (0.24 mmol g^{-1}, Rapp Polymere GmbH, Tuebingen, Germany) as solid support. All amino acids were incorporated as standard Fmoc amino acids, except His1 and Phe6-Thr7, which were incorporated as Boc-His(Trt)-OH and as the pseudoproline Fmoc-L-Phe-L-Thr-[PSI(Me,Me)Pro]-OH, respectively. Side-chain protecting groups for Fmoc amino acids were *tert*-butyl (*t*Bu, for Glu, Asp, Ser, Thr, Tyr), 2,2,4,6,7-pentamethyldihydrobenzofuran-5-sulfonyl (Pbf, for Arg), and trityl (Trt, for Asn, Gln, His). Fmoc amino acids (4 equiv) were coupled using DIC (3.8 equiv) and OxymaPure (4 equiv) in DMF for 2 × 2 h at room temperature. N^{α}-Fmoc deprotections were performed using 20% piperidine in NMP for 3 min, followed by 20% piperidine in NMP for 22 min. Resins were washed with 2 × NMP, 2 × CH_2Cl_2, and 2 × NMP. Following completion of the backbone sequence, the resin was washed with anhydrous CH_2Cl_2 and the Alloc protecting group at Lys26 was selectively removed using $(PPh_3)_4Pd(0)$ (1 equiv) and borane dimethylamine complex (1.2 equiv) in anhydrous CH_2Cl_2 for 2 h at room temperature. The neoglycolipids were then assembled on the partially deprotected peptidyl-resin. Fmoc-Muc-OH (4 equiv), Fmoc-Glu-OtBu (4 equiv), Fmoc-O2Oc-OH (4 equiv), C16 (4

DOI: 10.1021/acs.molpharmaceut.6b00787
Mol. Pharmaceutics XXXX, XXX, XXX−XXX

Table 5. Analytical Data for Compounds 4−14[a]

			molecular mass (Da)				
				obsd			
compd no.	t_R (min)	purity (%)	calcd	$[M + H]^{2+}$	$[M + H]^{3+}$	$[M + H]^{4+}$	$[M + H]^{5+}$
4	3.5	95	3297.7	1649.8	1100.3	825.8	660.8
5	3.5	95	3383.7	1693.4	1129.0	847.1	
6	4.5	99	3622.2	1812.4	1208.4	906.6	
7	4.4	99	3751.3	1876.5	1251.3	938.8	751.3
8	4.4	99	3985.6		1329.9	997.4	798.1
9	4.4	99	4013.5	2008.3	1338.9	1004.6	
10	4.6	99	4041.6	2022.2	1348.5	1011.6	
11	4.3	99	4219.7	2111.7	1408.0	1056.3	
12	4.4	99	4247.8		1417.2	1063.2	850.7
13	4.6	99	4275.8		1426.5	1070.3	856.5
14	4.4	99	3896.4	1948.9	1299.6	975.1	

[a]Retention time and purity are derived from analytical RP-HPLC using a C18 column. Calcd, calculated; obsd, observed.

equiv), C18 (4 equiv), and C20 (4 equiv) were coupled by hand using DIC (3.8 equiv) and OxymaPure (4 equiv) in DMF for 2 × 4−16 h at room temperature. N^{α}-Fmoc deprotections were performed using 20% piperidine in NMP for 5 min, followed by 20% piperidine in NMP for 25 min. Resins were washed with 3 × NMP, 3 × CH_2Cl_2, and 3 × NMP. Peptide release from the solid support and removal of acid-labile side-chain protecting groups was performed by treatment with TFA:TES:H_2O cleavage mixture (95:2.5:2.5, 5 mL) for 2 h. The resins were washed with additional TFA (5 mL), and the crude peptides were precipitated using Et_2O (40 mL) followed by centrifugation for 5 min at 4400 rpm. The crude peptides were redissolved in DMF and purified by preparative RP-HPLC. RP-HPLC fractions were analyzed by LC−MS, and fractions containing the acetylated peptides were collected and lyophilized to provide the acetylated peptides. Removal of the Ac protecting groups was accomplished by dissolving the peptides in CH_3OH to a concentration of approximately 1 mg mL^{-1} and adding $NaOCH_3$ (0.5 M) in CH_3OH (corresponding to 1% of the total volume). The reaction mixture was stirred for 30 min at room temperature and then quenched by addition of CH_3COOH (corresponding to 2% of the total volume). The reaction mixture was evaporated to dryness, redissolved in a mixture of CH_3COOH, H_2O, and CH_3CN (25:37.5:37.5), and purified by preparative RP-HPLC. RP-HPLC fractions were quantified by LC−MS, and fractions containing deacetylated peptide were collected and lyophilized to provide the final product. Analytical data are presented in Table 5.

Functional Screening. A HEK293 cell line with a stable expression of the EPAC cAMP-sensor as well as the GLP-1 receptor was utilized for functional assay. The cell line utilizes mCerulean and mCitrine attached to the EPAC protein as fluorescence resonance energy transfer (FRET) pair and was previously described by Mathiesen et al.[33] Cells were kept at 37 °C in DMEM growth medium supplemented with 10% heat-inactivated FBS and 1% penicillin−streptomycin in a humidified 5% CO_2 incubator. Furthermore, zeocin (0.05 mg mL^{-1}) and geneticin (0.5 mg mL^{-1}) were added to the growth medium to maintain selection pressure. On the day of measurement, cells were detached using nonenzymatic cell dissociation solution, spun down, and resuspended in assay buffer (HBSS with HEPES (20 mM) supplemented with $CaCl_2$ (1 mM), $MgCl_2$ (1 mM), and 0.1% albumin, pH 7.4) to a cell concentration of 105 cells mL^{-1}. Cells were then transferred to black 384-well microplates, where ligands were added in the indicated concentrations. Immediately afterwards, increases in cAMP levels were measured as increases in the mCerulean/mCitrine emission ratio using an Envision 2104 Multilabel Reader, with measurement starting from 1 min and continuing for 60 min after ligand addition. The energy donor mCerulean was excited using an optical filter CFP-430 (X430) and a CFP/YFP (D450_515) single mirror. Subsequently, emission from both the donor mCerulean and the acceptor mCitrine was measured using YFP-535 (M535) and CFP-470 (M470) filters. The 470 nm/535 nm emission ratio was plotted as a function of time. At the time point of maximum cAMP levels (approximately 30 min after addition of ligands), dose−response curves were generated and ligand EC50 values were calculated.

Assessment of Peptide Lipophilicity. Peptides were dissolved in a 1:1 mixture of H_2O and CH_3CN and analyzed by analytical RP-UPLC coupled to ESI-MS (Acquity UPLC/SQ, Waters) using a C18 column (Acquity UPLC BEH Amide column, 1.7 μm, 130 Å, 2.1 mm × 100 mm, Waters) and a solvent system consisting of buffer C and buffer D. Peptides were eluted from the column by isocratic elution with buffer D (0−1 min, 0−42%; 1−20 min, 42%; 20−20.5 min, 42−100%; 20.5−22.5 min, 100%; flow, 0.5 mL min^{-1}).

Assessment of Peptide Solubility. Peptides were dissolved in 1 mL of PBS (pH 7.4) until a saturated solution was obtained. Samples (n = 1 per peptide) were sonicated for 1 h, and the pH value was readjusted to 7.4 using aqueous NaOH (0.1 M). Samples were stored overnight at room temperature and centrifuged for 15 min at 4400 rpm, and the absorbance at 280 nm (A280) of the supernatant was measured using a NanoDrop 1000 (Thermo Scientific, Waltham, MA, USA). Molar concentration was calculated from the Beer−Lambert law (l = 1 cm, ε_{280} = 6970 M^{-1} cm^{-1} for all compounds). The supernatants were subsequently analyzed by SEC and DLS within 24 h.

Size Exclusion Chromatography. Samples (100 μL) were size-separated by FPLC (ÄKTAPurifier100, GE Healthcare) on a calibrated Superdex 75 10/300 column (Pharmacia, Uppsala, Sweden) at 10 °C using PBS (pH 7.4) as running buffer and a flow rate of 0.45 mL min^{-1}. Column eluate was monitored at 280 nm using an UV detector. Molecular weight standards were purchased from GE Healthcare (aprotinin, ribonuclease, carbonic anhydrase, and ovalbumin) and Sigma-Aldrich

DOI: 10.1021/acs.molpharmaceut.6b00787
Mol. Pharmaceutics XXXX, XXX, XXX−XXX

(vitamin B12) or produced in-house (PYY3−36). Apparent molecular weight was calculated from molecular weight standards using a linear calibration curve generated from a plot of retention volume versus log(MW) (Figure S2). For clarity, peak height was normalized to 1 for all compounds.

Dynamic Light Scattering. Samples (300−500 μL) were filtered through a 0.2 μm syringe filter (Whatman Anotop Plus, GE Healthcare, Chicago, IL, USA) and placed in a quartz cuvette. Samples were analyzed using an instrument consisting of a BI-200SM goniometer, a BI-APD Avalanche photodiode detector, a BI-9000AT digital autocorrelator, and a 632.8 nm HeNe laser with a power of 35 mW (Brookhaven Instruments Corp., NY, USA). All measurements were obtained at 25 °C as 4−8 acquisitions of 60 s. Data were analyzed using software provided by Brookhaven Instruments (9KDSLW). A regularization algorithm was used to establish the presence of a monomodal size distribution, and cumulant analysis was used to estimate the average hydrodynamic radius (r_H) of the particles via the Stokes−Einstein equation. The reported values of r_H are derived from the data fit generated by second-order cumulant analysis.

Albumin Binding. SPR experiments were conducted on a Biacore X100 optical biosensor equipped with a CM5 chip (Biacore AB, GE Healthcare, Uppsala, Sweden). All buffers and reagents were filtered through a 0.2 μm filter and degassed by sonication for at least 30 min prior to use. HSA (fatty acid free) was immobilized by amine-coupling chemistry according to Rich et al.[34] The CM5 chip was docked and primed 5−10 times with running buffer (PBS, pH 7.4). The chip was activated by injecting a 1:1 mixture of 3-(*N*,*N*-dimethylamino)propyl-*N*-ethylcarbodiimide (EDC, 0.4 M) and *N*-hydroxysuccinimide (NHS, 0.1 M) in PBS buffer pH 7.4 to both flow cells 1 and 2 for 2 × 7 min at 25 °C at a flow rate of 10 μL min^{-1}. Immobilization was conducted by injecting fatty acid free HSA (30 μg/mL) dissolved in NaOAc buffer (10 mM, pH 5.2) to flow cell 2 for 2 × 7 min at 25 °C at a flow rate of 10 μL min^{-1}. After immobilization, the chip was blocked and washed by injection of ethanolamine (1 M) to flow cells 1 and 2 for 2 × 3 min at 25 °C at a flow rate of 30 μL/min, followed by injection of NaOH (50 mM) to flow cells 1 and 2 for 3 × 12 s at 25 °C at a flow rate of 30 μL min^{-1}. The procedure resulted in immobilization of HSA on flow cell 2 corresponding to approximately 8300 RU. Binding analysis was performed using PBS (pH 7.4) containing 3% DMSO as running buffer. For each compound, a sample series containing 50, 25, and 5 μM samples was prepared by making a 50 μM stock solution followed by dilution with running buffer to avoid bulk shift effects. All compounds were analyzed twice (n = 2), with all samples being injected in triplicate with the lowest concentration being analyzed first to prevent carryover effects. All samples were injected through both flow cells 1 and 2 to allow double referencing (i.e., subtraction of the inherent SPR response from the reference surface as well as the running buffer). Each sample cycle consisted of an association phase (sample injection for 150 s at 30 μL min^{-1}), a dissociation phase (running buffer injection for 180 s at 30 μL min^{-1}), and a regeneration step (injection of 50 mM NaOH for 4 s at 30 μL min^{-1}). After each sample series, a blank injection was included in order to visualize any compound carryover. Data was analyzed by nonlinear regression using the Association then Dissociation model (constraints: HotNM = data set constant (=column title); k_{on} = Shared value for all data sets; k_{off} = Shared value for all data sets; Time0 = Constant equal to 145). Data plot represents mean ± SEM of a single representative experiment with triplicate injections. The reported values of k_d, $k_{a,app}$ and $K_{D,app}$ are reported as mean ± SEM, n = 2.

Animal Welfare. Animal experiments were conducted in accordance with internationally accepted principles for the care and use of laboratory animals and were covered by a personal license issued for Jacob Jelsing (permit number: 2013-15-2934-00784, approved by the Danish Committee for Animal Research). Mice (male NMRI mice, each weighing approximately 30 g) were obtained from Taconic (Lille Skensved, Denmark). The mice were housed in groups of four in a light-controlled, temperature-controlled, and humidity-controlled room (a 12/12 light−darkness cycle, lights on at 2:00 a.m.; 22 ± 2 °C; 50% relative humidity). During experiments, the mice had ad libitum access to regular chow diet (Altromin 1324, Brogaarden A/S, Lynge, Denmark) and domestic quality tap water.

Acute Effect on Glucose Tolerance. The effect on glucose homeostasis of compounds **8**−**10** was evaluated in comparison with liraglutide and vehicle (5 mL kg^{-1}, consisting of PBS (pH 7.4) containing 0.1% BSA in an oral glucose tolerance test (OGTT). Male NMRI mice (each weighing 25−30 g) were acclimatized for a minimum of 5 days. Prior to entering the experiment, animals are randomized into treatment groups according to body weight. On the day of experiment, animals were fasted for 3 h prior to compound administration (sc, 50 nmol kg^{-1}) at t = −45 min. At t = 0, animals are given an oral glucose load (2 g kg^{-1}; dose volume 10 mL kg^{-1}; glucose solution 200 mg mL^{-1}, Fresenius Kabi, Sweden). Blood samples were drawn from the tail vein at time points −45, 0, 15, 30, 60, and 120 min, collected into 10 μL heparinized glass capillary tubes, and immediately suspended in buffer (0.5 mL of glucose/lactate system solution, EKF-diagnostics, Germany) and analyzed for glucose on the test day using a BIOSEN c-Line glucose meter (EKF-diagnostics, Germany) according to the manufacturer's instructions. Statistical analysis was performed using one-way analysis of variance (ANOVA) followed by Bonferroni's post test against vehicle (p < 0.05 for statistical significance). Data are presented as mean ± SEM, n = 7.

Acute Effect on Food Intake. Food intake was measured using a fully automated food intake monitoring system (HM-2; MBRose ApS, Faaborg, Denmark) allowing for real-time monitoring of food intake behavior of individual animals as described in details by Axel et al.[35] Upon arrival, the mice were transferred to the HM-2 system, acclimatized to their new environment for a minimum of 5 days, and handled daily to accustom them to the experimental paradigm. Mice were uniquely identified with sc implantable microchips (Pet ID Microchip, E-vet, Haderslev, Denmark) to allow identification of each individual upon entry and exit from the food channel. On the day of dosing, animals were randomized into treatment groups according to body weight, and the acute anorectic effect of compounds **8**, **9**, **11**, and **12** was evaluated in comparison with liraglutide and vehicle (5 mL kg^{-1}, consisting of PBS (pH 7.4) containing 0.1% BSA. Mice were dosed sc in the lower back (dose, 50 nmol kg^{-1}; dose volume, 5 mL kg^{-1}) in the afternoon just prior to lights out, and food intake data were collected for 18 h post dosing. Data were obtained from two independent studies. The first study contained the following treatment groups: vehicle (n = 6), liraglutide (n = 8), **8** (n = 6), **9** (n = 7), and **12** (n = 8). The second study contained the following groups: vehicle (n = 9), **8** (n = 9), **9** (n = 9), **11** (n =

DOI: 10.1021/acs.molpharmaceut.6b00787
Mol. Pharmaceutics XXXX, XXX, XXX−XXX

9), and **12** (n = 9). All data from the two studies were pooled prior to analysis. Statistical analysis was performed using a one-way ANOVA followed by Dunnett's multiple comparison test (p < 0.05 for statistical significance). Data are presented as mean ± SEM, n = 8−17.

■ ASSOCIATED CONTENT

Supporting Information

The Supporting Information is available free of charge on the ACS Publications website at DOI: 10.1021/acs.molpharmaceut.6b00787.

Synthesis strategy for neoglycolipidated peptides, SEC calibration curve, and additional kinetic data from Biacore experiments (PDF)

■ AUTHOR INFORMATION

Corresponding Authors

*E-mail: kjj@chem.ku.dk. Phone: +4535332430.
*E-mail: slp@gubra.dk. Phone: +4531522650.

ORCID

Knud J. Jensen: 0000-0003-3525-5452

Author Contributions

S.B.v.W., K.M., P.W., and E.M.B. performed the experiments. S.B.v.W., K.M., M.B.T., N.V., J.J., K.J.J., and S.L.P discussed the data. S.B.v.W., M.B.T., K.J.J., and S.L.P. wrote the manuscript.

Notes

The authors declare the following competing financial interest(s): Niels Vrang and Jacob Jelsing are major shareholders in Gubra ApS.

■ ACKNOWLEDGMENTS

The authors thank Lena Hansen for synthesis of GLP-1(7-36)-NH_2 (**4**) and PYY3-36, Dr. Jesper Mosolff Mathiesen for providing the HEK293 cell line used for functional screening, and Dr. Søren Roi Midtgaard for aiding with SEC and DLS experiments. Mie Fabricius Wöldike and Prof. Hans Bräuner-Osborne are thanked for providing the facilities for conducting the functional assays. The authors wish to acknowledge the Innovation Fund Denmark for cofinancing PhD stipends to S.B.v.W. (Grant No. 1355-00066B), P.W. (Grant No. 4135-00073B), and E.M.B. (Grant No. 5016-00132B).

■ ABBREVIATIONS USED

ANOVA, analysis of variance; C16, palmitic acid; C18, stearic acid; C20, arachidic acid; DIC, *N*,*N*′-diisopropylcarbodiimide; DIPEA, *N*,*N*-diisopropylethylamine; DLS, dynamic light scattering; DMEM, Dulbecco's modified Eagle medium; EDA, ethylenediamine; EDC, 3-(*N*,*N*-dimethylamino)propyl-*N*-ethylcarbodiimide; ESI-MS, electrospray ionization mass spectrometry; FBS, fetal bovine serum; Fmoc, 9-fluorenylmethyloxycarbonyl; FRET, fluorescence resonance energy transfer; HBSS, Hanks balanced salt solution; HEPES, 4-(2-hydroxyethyl)-1-piperazineethanesulfonic acid; HM-2, HerdsMan-2; HSA, human serum albumin; k_a, association rate constant; k_d, dissociation rate constant; K_D, equilibrium dissociation constant; m, oligomeric state; NHS, *N*-hydroxysuccinimide; NMP, *N*-methyl-2-pyrrolidone; OGTT, oral glucose tolerance test; OxymaPure, ethyl (hydroxyimino)cyanoacetate; Pbf, 2,2,4,6,7-pentamethyldihydrobenzofuran-5-sulfonyl; PI, polydispersity index; RU, response unit; SEC, size exclusion chromatography; SPR, surface plasmon resonance; SPPS, solid-phase peptide synthesis; SLS, static light scattering; V_R, retention volume

■ REFERENCES

(1) Walsh, G. Biopharmaceutical benchmarks 2014. *Nat. Biotechnol.* **2014**, *32* (10), 992−1000.
(2) Kontermann, R. E. Strategies for extended serum half-life of protein therapeutics. *Curr. Opin. Biotechnol.* **2011**, *22* (6), 868−876.
(3) Kontermann, R. Half-Life Modulating Strategies—An Introduction. In *Therapeutic Peptides: Strategies to Modulate Their Plasma Half-Lives*; Kontermann, R., Ed.; Wiley-Blackwell: Weinheim, 2012; pp 3−21.
(4) Pelegri-O'Day, E. M.; Lin, E. W.; Maynard, H. D. Therapeutic Protein-Polymer Conjugates: Advancing Beyond PEGylation. *J. Am. Chem. Soc.* **2014**, *136* (41), 14323−14332.
(5) van Witteloostuijn, S. B.; Pedersen, S. L.; Jensen, K. J. Half-Life Extension of Biopharmaceuticals using Chemical Methods - Alternatives to PEGylation. *ChemMedChem* **2016**, *11*, 2474.
(6) Vernet, E.; Popa, G.; Pozdnyakova, I.; Rasmussen, J. E.; Grohganz, H.; Giehm, L.; Jensen, M. H.; Wang, H.; Plesner, B.; Nielsen, H. M.; Jensen, K. J.; Berthelsen, J.; Sundström, M.; van de Weert, M. Large-Scale Biophysical Evaluation of Protein PEGylation Effects: In Vitro Properties of 61 Protein Entities. *Mol. Pharmaceutics* **2016**, *13* (5), 1587−1598.
(7) Harris, J. M.; Chess, R. B. Effect of pegylation on pharmaceuticals. *Nat. Rev. Drug Discovery* **2003**, *2* (3), 214−21.
(8) Pasut, G.; Veronese, F. M. State of the art in PEGylation: The great versatility achieved after forty years of research. *J. Controlled Release* **2012**, *161* (2), 461−472.
(9) Pasut, G. Polymers for Protein Conjugation. *Polymers* **2014**, *6* (1), 160−178.
(10) Knop, K.; Hoogenboom, R.; Fischer, D.; Schubert, U. S. Poly(ethylene glycol) in drug delivery: pros and cons as well as potential alternatives. *Angew. Chem., Int. Ed.* **2010**, *49* (36), 6288−308.
(11) Havelund, S.; Plum, A.; Ribel, U.; Jonassen, I.; Vølund, A.; Markussen, J.; Kurtzhals, P. The Mechanism of Protraction of Insulin Detemir, a Long-acting, Acylated Analog of Human Insulin. *Pharm. Res.* **2004**, *21* (8), 1498−1504.
(12) Jonassen, I.; Havelund, S.; Hoeg-Jensen, T.; Steensgaard, D. B.; Wahlund, P. O.; Ribel, U. Design of the novel protraction mechanism of insulin degludec, an ultra-long-acting basal insulin. *Pharm. Res.* **2012**, *29* (8), 2104−2014.
(13) Madsen, K.; Knudsen, L. B.; Agersoe, H.; Nielsen, P. F.; Thøgersen, H.; Wilken, M.; Johansen, N. L. Structure-Activity and Protraction Relationship of Long-Acting Glucagon-like Peptide-1 Derivatives: Importance of Fatty Acid Length, Polarity, and Bulkiness. *J. Med. Chem.* **2007**, *50*, 6126−6132.
(14) Lau, J.; Bloch, P.; Schaffer, L.; Pettersson, I.; Spetzler, J.; Kofoed, J.; Madsen, K.; Knudsen, L. B.; McGuire, J.; Steensgaard, D. B.; Strauss, H. M.; Gram, D. X.; Knudsen, S. M.; Nielsen, F. S.; Thygesen, P.; Reedtz-Runge, S.; Kruse, T. Discovery of the Once-Weekly Glucagon-Like Peptide-1 (GLP-1) Analogue Semaglutide. *J. Med. Chem.* **2015**, *58* (18), 7370−7380.
(15) Kurtzhals, P.; Havelund, S.; Jonassen, I.; Kiehr, B.; Larsen, U. D.; Ribel, U.; Markussen, J. Albumin binding of insulins acylated with fatty acids: characterization of theligand-protein interaction and correlation between binding affinity and timing of the insulin effect in vivo. *Biochem. J.* **1995**, *312*, 725−731.
(16) Markussen, J.; Havelund, S.; Kurtzhals, P.; Andersen, A. S.; Halstrom, J.; Hasselager, E.; Larsen, U. D.; Ribel, U.; Schaffer, L.; Vad, K.; Jonassen, I. Soluble, fatty acid acylated insulins bind to albumin and show protracted action in pigs. *Diabetologia* **1996**, *39* (3), 281−288.
(17) Myers, S. R.; Yakubu-Madus, F. E.; Johnson, W. T.; Baker, J. E.; Cusick, T. S.; Williams, V. K.; Tinsley, F. C.; Kriauciunas, A.; Manetta, J.; Chen, V. J. Acylation of Human Insulin With Palmitic Acid Extends the Time Action of Human Insulin in Diabetic Dogs. *Diabetes* **1997**, *46*, 637−642.

DOI: 10.1021/acs.molpharmaceut.6b00787
Mol. Pharmaceutics XXXX, XXX, XXX−XXX

(18) Steensgaard, D. B.; Thomsen, J. K.; Olsen, H. B.; Knudsen, L. B. The Molecular Basis for the Delayed Absorption of the Once-Daily Human GLP-1 Analog, Liraglutide. *Diabetes* **2008**, *57* (Suppl. 1), A164.
(19) Day, J. W.; Ottaway, N.; Patterson, J. T.; Gelfanov, V.; Smiley, D.; Gidda, J.; Findeisen, H.; Bruemmer, D.; Drucker, D. J.; Chaudhary, N.; Holland, J.; Hembree, J.; Abplanalp, W.; Grant, E.; Ruehl, J.; Wilson, H.; Kirchner, H.; Lockie, S. H.; Hofmann, S.; Woods, S. C.; Nogueiras, R.; Pfluger, P. T.; Perez-Tilve, D.; DiMarchi, R.; Tschöp, M. H. A new glucagon and GLP-1 co-agonist eliminates obesity in rodents. *Nat. Chem. Biol.* **2009**, *5* (10), 749−757.
(20) Bellmann-Sickert, K.; Elling, C. E.; Madsen, A. N.; Little, P. B.; Lundgren, K.; Gerlach, L. O.; Bergmann, R.; Holst, B.; Schwartz, T. W.; Beck-Sickinger, A. G. Long-acting lipidated analogue of human pancreatic polypeptide is slowly released into circulation. *J. Med. Chem.* **2011**, *54* (8), 2658−67.
(21) Whittingham, J. L.; Havelund, S.; Jonassen, I. Crystal structure of a prolonged-acting insulin with albumin-binding properties. *Biochemistry* **1997**, *36* (10), 2826−2831.
(22) Finan, B.; Ma, T.; Ottaway, N.; Muller, T. D.; Habegger, K. M.; Heppner, K. M.; Kirchner, H.; Holland, J.; Hembree, J.; Raver, C.; Lockie, S. H.; Smiley, D. L.; Gelfanov, V.; Yang, B.; Hofmann, S.; Bruemmer, D.; Drucker, D. J.; Pfluger, P. T.; Perez-Tilve, D.; Gidda, J.; Vignati, L.; Zhang, L.; Hauptman, J. B.; Lau, M.; Brecheisen, M.; Uhles, S.; Riboulet, W.; Hainaut, E.; Sebokova, E.; Conde-Knape, K.; Konkar, A.; DiMarchi, R. D.; Tschöp, M. H. Unimolecular dual incretins maximize metabolic benefits in rodents, monkeys, and humans. *Sci. Transl. Med.* **2013**, *5* (209), 209ra151.
(23) Dalbøge, L. S.; Pedersen, S. L.; van Witteloostuijn, S. B.; Rasmussen, J. E.; Rigbolt, K. T.; Jensen, K. J.; Holst, B.; Vrang, N.; Jelsing, J. Synthesis and evaluation of novel lipidated neuromedin U analogs with increased stability and effects on food intake. *J. Pept. Sci.* **2015**, *21* (2), 85−94.
(24) Seddon, A. M.; Curnow, P.; Booth, P. J. Membrane proteins, lipids and detergents: not just a soap opera. *Biochim. Biophys. Acta, Biomembr.* **2004**, *1666* (1−2), 105−117.
(25) Holst, J. J. The physiology of glucagon-like peptide 1. *Physiol. Rev.* **2007**, *87* (4), 1409−39.
(26) Lorenz, M.; Evers, A.; Wagner, M. Recent progress and future options in the development of GLP-1 receptor agonists for the treatment of diabesity. *Bioorg. Med. Chem. Lett.* **2013**, *23* (14), 4011−8.
(27) Meier, J. J. GLP-1 receptor agonists for individualized treatment of type 2 diabetes mellitus. *Nat. Rev. Endocrinol.* **2012**, *8* (12), 728−42.
(28) Knudsen, L. B.; Nielsen, P. F.; Huusfeldt, P. O.; Johansen, N. L.; Madsen, K.; Pedersen, F. Z.; Thøgersen, H.; Wilken, M.; Agersø, H. Potent Derivatives of Glucagon-like Peptide-1 with Pharmacokinetic Properties Suitable for Once Daily Administration. *J. Med. Chem.* **2000**, *43*, 1664−1669.
(29) Wang, Y.; Lomakin, A.; Kanai, S.; Alex, R.; Benedek, G. B. Transformation of Oligomers of Lipidated Peptide Induced by Change in pH. *Mol. Pharmaceutics* **2015**, *12* (2), 411−419.
(30) Clodfelter, D. K.; Pekar, A. H.; Rebhun, D. M.; Destrampe, K. A.; Havel, H. A.; Myers, S. R.; Brader, M. L. Effects of non-covalent self-association on the subcutaneous absorption of a therapeutic peptide. *Pharm. Res.* **1998**, *15* (2), 254−262.
(31) Plum, A.; Jensen, L. B.; Kristensen, J. B. In vitro protein binding of liraglutide in human plasma determined by reiterated stepwise equilibrium dialysis. *J. Pharm. Sci.* **2013**, *102* (8), 2882−2888.
(32) Dangschat, G.; Fischer, H. O. L. The Configuration of Conduritol and the Synthesis of Muco-Inositol and Allo-Inositol. *Carbohydr. Res.* **1987**, *164*, 343−355.
(33) Mathiesen, J. M.; Vedel, L.; Brauner-Osborne, H. cAMP Biosensors Applied in Molecular Pharmacological Studies of G Protein-Coupled Receptors. In *G Protein Coupled Receptors: Modeling, Activation, Interactions and Virtual Screening*; Conn, P. M., Ed.; Elsevier Academic Press Inc.: San Diego, 2013; Vol. *522*, pp 191−207.
(34) Rich, R. L.; Day, Y. S. N.; Morton, T. A.; Myszka, D. G. High-resolution and high-throughput protocols for measuring drug/human serum albumin interactions using BIACORE. *Anal. Biochem.* **2001**, *296* (2), 197−207.
(35) Axel, A. M. D.; Mikkelsen, J. D.; Hansen, H. H. Tesofensine, a Novel Triple Monoamine Reuptake Inhibitor, Induces Appetite Suppression by Indirect Stimulation of alpha(1) Adrenoceptor and Dopamine D-1 Receptor Pathways in the Diet-Induced Obese Rat. *Neuropsychopharmacology* **2010**, *35* (7), 1464−1476.

DOI: 10.1021/acs.molpharmaceut.6b00787
Mol. Pharmaceutics XXXX, XXX, XXX−XXX